JOURNAL OF COMPUTATIONAL PHYSICS 33, 153–168 (1979)

Finite Difference Analysis of Surface Acoustic Wave Propagation and Scattering in Piezoelectric Crystals

E. CAMBIAGGIO

Department of Electronics, University of Nice, Parc Valrose, 06034 Nice Cedex, France

AND

F. CUOZZO

University of Toulon, Château Saint Michel, R.N. 98, 83130 La Garde, France

Received July 17, 1978; revised November 8, 1978

A finite difference analysis of surface acoustic wave propagation and scattering in piezoelectric crystals is presented. Numerical solutions of coupled electromechanical equations are obtained from an association of a recursive technique with linear iterative methods. Finite difference approximations are presented for various surface perturbations, and numerical simulations are achieved for some electrical discontinuities on the surface of a $LiNbO_3$ crystal.

1. INTRODUCTION

The propagation of acoustic surface waves on solids is a physical phenomenon widely used nowadays in the realization of simple and compact surface acoustic wave (SAW) devices [1] which perform various signal processing functions in the megahertz to gigahertz range of frequencies. Most of these SAW devices are built on piezoelectric crystals allowing very simple techniques for the realization of electromechanical transducers.

However, while the SAW propagation on piezoelectric crystals is well known for the simplest geometries such as the infinite free surface, the infinite metallized surface, or the infinite layered media [2], accurate analytical solutions are not available when the geometry becomes more complex. This case occurs, for instance, when metallic strips are layered on the surface. Every discontinuity between a free surface region and a metallized one scatters the acoustic wave. This scattering phenomenon, which is undesirable when it distubs the component function, may on the other hand be useful in some other devices, such as reflectors, resonators, etc. In any event, a better knowledge of scattering phenomena is necessary, both to avoid parasitic reflections from transducers and to design optimal geometries of reflectors.

0021-9991/79/110153-16$02.00/0

The problem of SAW propagation and scattering is governed by partial differential equations with boundary conditions; thus finite difference techniques are particularly suited to finding solutions of such a problem. These techniques have been successfully used by several authors [3–11], who have determined the surface wave scattering from various geometrical obstacles but only on isotropic solids.

In this paper, we propose a finite difference analysis of surface wave propagation and scattering on high coupling piezoelectric substrates. This method is more complete than the earlier ones, because it takes into account anisotropy, piezoelectricity, and electrical boundary conditions. In order to solve the coupled equations in piezoelectric materials, the association of two different techniques using finite difference approximations is required:

(a) The initial value problem for the mechanical displacements [12, 13] is solved by recursive techniques.

(b) At every step of the recursive process, Dirichlet's problem of the electrical potential is solved by linear iterative techniques [13, 14].

This method has been used for the study of electrical discontinuities, i.e., the effect of short-circuiting some regions of the crystal surface and results concerning both surface wave behavior and electrical behavior have been determined. Some of these results have been presented already [15–17].

2. Statement of the Problem

Figure 1 shows a longitudinal section of a part of a SAW device. The surface wave, which propagates along the direction x_1, meets finite width metallic layers S_1, S_2,.... These metallic layers are assumed to be massless and perfectly conducting.

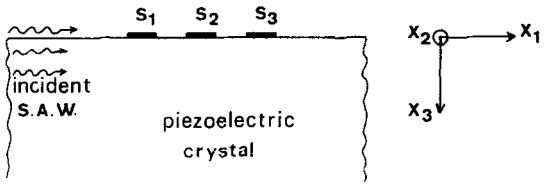

FIG. 1. Longitudinal section of a part of an SAW device. The incident surface wave, propagating in the direction x_1, meets metallic layers S_1, S_2, S_3.

This approximation is valid when thin layers of a light metal are layered on the surface of a high coupling piezoelectric crystal: When the layer thickness is small enough with regard to surface wave wavelength, the mechanical effects (mass loading) may be neglected with regard to short-circuit effects [18, 19] (for example, *Al* electrodes on $LiNbO_3$, and frequencies up to about 100 MHz).

The electromechanical system is governed by the following partial differential equations [2, 20, 21].

(a) *In the piezoelectric crystal.*

—Equation of motion (hyperbolic)

$$\rho \frac{\partial^2 u_j}{\partial t^2} = c_{ijkl} \frac{\partial^2 u_k}{\partial x_i \partial x_l} - e_{kij} \frac{\partial^2 V}{\partial x_k \partial x_i}, \qquad i, j, k, l = 1, 2, 3. \tag{1}$$

—Equation of piezoelectric coupling (elliptic)

$$e_{ikl} \frac{\partial^2 u_k}{\partial x_i \partial x_l} - \epsilon_{ik} \frac{\partial^2 V}{\partial x_k \partial x_i} = 0, \qquad i, k, l = 1, 2, 3, \tag{2}$$

where the u_i are the mechanical displacement components, measured along the Cartesian axes to which the stiffness tensor c_{ijkl}, the piezoelectric tensor e_{kij}, and the dielectric tensor ϵ_{ik} are referred, V is the electrical potential, and ρ is the density of the crystal.

(b) *In the vacuum.* Laplace's equation (elliptic)

$$\nabla^2 V = 0. \tag{3}$$

(c) *Boundary conditions.* The boundary conditions take into account the local conditions on the surface (i.e., free surface or short circuited surface). One can consider two kinds of conditions:

—Mechanical boundary conditions: The surface must be traction-free e.c.

$$T_{3j} = c_{3jkl} \frac{\partial u_k}{\partial x_l} + e_{k3j} \frac{\partial V}{\partial x_k} = 0 \qquad \text{for} \quad x_3 = 0, \tag{4}$$

where T_{3j} are elements of the stress tensor. Since the metal strips have been assumed massless (very thin plating), this condition must be imposed even for a metalized surface.

—Electrical boundary conditions: For a free surface, the electrical potential V and the normal component D_3 of electrical displacement must be continuous across the charge-free interface. Furthermore, the potential must vanish when $x_3 \to -\infty$

$$V(x_3 = 0^+) = V(x_3 = 0^-), \tag{5}$$

$$D_3(x_3 = 0^+) = D_3(x_3 = 0^-), \tag{6}$$

with

$$D_3 = -\epsilon_0 \frac{\partial V}{\partial x_3} \qquad \text{for} \quad x_3 \leqslant 0, \tag{7}$$

$$D_3 = e_{3kl} \frac{\partial u_k}{\partial x_l} - \epsilon_{3k} \frac{\partial V}{\partial x_k} \qquad \text{for} \quad x_3 \geqslant 0. \tag{8}$$

For a short-circuited surface, the electrical boundary condition must be

$$\frac{\partial V}{\partial x_1} = 0, \qquad \text{for} \quad x_3 = 0. \tag{9}$$

Finite difference techniques are particularly suited to solving such problems, but they require important computing resources. In this first step, we have achieved a finite difference analysis of the behavior of an incident straight-crested Rayleigh wave in the particular case of Z propagation on Y-cut $LiNbO_3$ crystal.

This particular cut on $LiNbO_3$ has been chosen both for its high piezoelectric coupling constant [22–24] and for the characteristics of the Z-propagating Rayleigh wave, which has only two displacement components. Nevertheless, this analysis is suitable for other Y-cut Z-propagating crystals of class $3m$, like $LiTaO_3$, for example.

3. Finite Difference Analysis

The invariance of solutions along x_2 for staight-crested waves allows us to consider only two spatial variables, x_1 and x_3. Z-propagating Rayleigh waves on a Y-cut $LiNbO_3$ crystal have no transverse displacement component u_2. Furthermore, some elements of the stiffness, piezoelectric, and dielectric tensors are null [25, 26]. Thus, the problem is reduced to three variables (x_1, x_3, and time) and solutions will be searched only for the displacements u_1 and u_3 and for the potential V.

3.1. *Discretization*

A closed study domain $ABCD$ is chosen (Fig. 2) into which both time and space variables are discretized by superimposing a square grid on the domain $ABCD$, with a mesh spacing h. Each node located at $x_1 = ih$ and $x_3 = jh$ is characterized by the set of integer indices (i, j) where i and j are increasing, respectively, along x_1 and x_3. The domain has M nodes along x_1 and N nodes along x_3 [$AB = (M - 1)h$ and $AD = (N - 1)h$]. The time increment is denoted by l, and the time $\tau = tl$ is characterized by the integer index t.

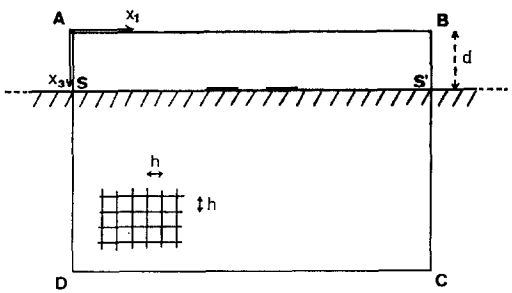

Fig. 2. The space is discretized into the study domain $ABCD$. (The mesh spacing $\Delta x_1 = \Delta x_3 = h$.)

3.2. *Determination of Mechanical Displacements*

(a) The centered finite difference approximation of the equation of motion (1) can be written

$$\begin{aligned}\overline{U}'(i,j,t+1) = {} & 2\overline{U}'(i,j,t) - \overline{U}'(i,j,t-1) \\ & + [A][\overline{U}(i+1,j,t) - 2\overline{U}(i,j,t) + \overline{U}(i-1,j,t)] \\ & + [B][\overline{U}(i,j+1,t) - 2\overline{U}(i,j,t) + \overline{U}(i,j-1,t)] \\ & + [C][\overline{U}(i+1,j+1,t) + \overline{U}(i-1,j-1,t) \\ & - \overline{U}(i+1,j-1,t) - \overline{U}(i-1,j+1,t)], \end{aligned} \tag{10}$$

where

$$\overline{U}(i,j,t) = \begin{bmatrix} u_1(i,j,t) \\ u_3(i,j,t) \\ V(i,j,t) \end{bmatrix} \quad \text{and} \quad \overline{U}'(i,j,t) = \begin{bmatrix} u_1(i,j,t) \\ u_3(i,j,t) \end{bmatrix}, \tag{11, 12}$$

$$[A] = \frac{l^2}{\rho h^2}\begin{bmatrix} c_{11} & 0 & e_{11} \\ 0 & c_{55} & 0 \end{bmatrix}, \tag{13}$$

$$[B] = \frac{l^2}{\rho h^2}\begin{bmatrix} c_{55} & c_{35} & e_{35} \\ c_{35} & c_{33} & e_{33} \end{bmatrix}, \tag{14}$$

$$[C] = \frac{l^2}{4\rho h^2}\begin{bmatrix} 0 & (c_{13}+c_{35}) & 0 \\ (c_{13}+c_{35}) & 2c_{35} & (e_{13}+e_{35}) \end{bmatrix}, \tag{15}$$

where c_{ij} and e_{ij} are components of the matrix form of the stiffness and piezoelectric tensors (obtained by the Voigt notation) [26].

The two explicit difference equations obtained from (10) allow the determination of the displacement of the node (i,j) at time $(t+1)$ as a linear combination of displacements and potentials of node (i,j) and its eight neighbors at the two previous time levels (t) and $(t-1)$ (Fig. 3). However, these equations cannot be used to determine the displacements of nodes lying either on the artificial boundaries *ABCD* or on the free surface *SS'*, because these nodes do not have eight neighbors. The difficulty is eliminated on the artificial boundaries *ABCD* by imposing suitable values to corresponding nodes, but the physical boundary *SS'* requires a particular treatment.

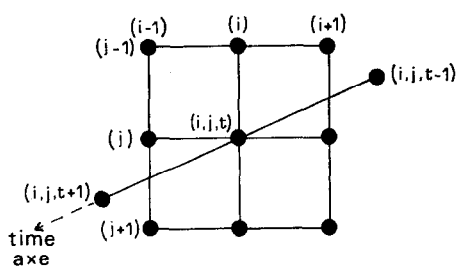

FIG. 3. Displacements of node (i,j) at time $t+1$ is a linear combination of displacements and potentials of node (i,j) and its eight neighbors at the two preceding times t and $t-1$.

(b) *Boundary conditions.* The nodes lying along the crystal surface SS' must satisfy the boundary conditions (4) and (5)–(9). In order to compute the mechanical displacements of surface nodes with the explicit finite difference equation (10), fictitious values of displacements and potentials are determined on the line located just above the surface (Fig. 4, line j–1). These fictitious values of potentials and displacements are such that the boundary conditions are satisfied on the surface line (j) [3–11]. (It should be noted that two values of potentials are avilable for nodes of line $j-1$: The actual value of potential in the vacuum and the fictitious one required by the boundary-condition expressions.)

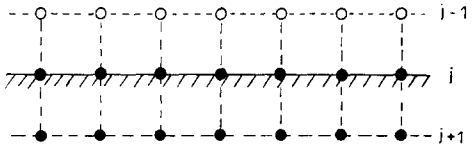

FIG. 4. On the nodes ○ of line $(j-1)$ above the surface, fictitious values of displacements and potentials are determined according to the boundary conditions.

From finite difference approximations of the boundary conditions, the fictitious electromechanical vector $U_f(i, j-1, t)$ for the node located at $(i, j-1)$ is determined.

$$U_f(i, j-1, t) = [M]^{-1} \begin{pmatrix} \alpha \\ \beta \\ \gamma \end{pmatrix}, \tag{16}$$

with

$$U_f(i, j-1, t) = \begin{bmatrix} u_1(i, j-1, t) \\ u_3(i, j-1, t) \\ V(i, j-1, t) \end{bmatrix} \quad \text{(fictitious values)}, \tag{17}$$

$$\alpha = c_{55}[u_1(i, j+1, t) + u_3(i+1, j, t) - u_3(i-1, j, t)] + c_{35}u_3(i, j+1, t) + e_{35}V(i, j+1, t), \tag{18}$$

$$\beta = c_{13}[u_1(i+1, j, t) - u_1(i-1, j, t)] + c_{35}[u_1(i, j+1, t) + u_3(i+1, j, t) - u_3(i-1, j, t)] + c_{33}u_3(i, j+1, t) + e_{13}[V(i+1, j, t) - V(i-1, j, t)] + e_{33}V(i, j+1, t). \tag{19}$$

Matrix $[M]$ and γ depend on electrical boundary conditions; for a free surface,

$$[M] = \begin{bmatrix} c_{55} & c_{35} & e_{35} \\ c_{35} & c_{33} & e_{33} \\ e_{35} & e_{33} & -\epsilon_{33} \end{bmatrix}, \tag{20}$$

$$\gamma = e_{35}[u_1(i, j+1, t) + u_3(i+1, j, t) - u_3(i-1, j, t)] + e_{33}u_3(i, j+1, t) - \epsilon_{33}V(i, j+1, t) - \epsilon_0[V(i+1, j, t) + V(i-1, j, t) + 2V(i, j-1, t) - 4V(i, j, t)], \tag{21}$$

and for a metallized surface,

$$[M] = \begin{bmatrix} c_{55} & c_{35} & e_{35} \\ c_{35} & c_{33} & e_{33} \\ 0 & 0 & 1 \end{bmatrix}, \tag{22}$$

$$\gamma = 2V(i, j, t) - V(i, j+1, t). \tag{23}$$

(c) *Stability conditions.* By the application of a standard von Neumann analysis analogous to the one presented by Alterman and Loewenthal [4] we get the necessary stability condition

$$\left(\frac{h}{l}\right)^2 > \frac{a + c + [(c+b)^2 + 4d]^{1/2}}{2\rho}, \tag{24}$$

with

$$a = c_{11} + c_{33} + 2c_{55}; \qquad b = c_{33} - c_{11}; \qquad c = \frac{e_{33}^2 + (e_{11} + e_{35})^2}{\epsilon_{11} + \epsilon_{33}};$$

$$d = c_{35}^2 + \frac{(e_{11} + e_{35})[2e_{33}c_{35} + (c_{11} - c_{33})(e_{11} + e_{35})]}{\epsilon_{11} + \epsilon_{33}},$$

which yields to

$$\begin{aligned} (h/l) &> 8546 \text{ m/sec for } YZ \text{ } LiNnO_3, \\ (h/l) &> 7332 \text{ m/sec for } YZ \text{ } LiTaO_3. \end{aligned} \tag{25}$$

Usually, we have chosen h/l about 20% higher than the minimal value of (25). However, this von Neumann condition applies only for nodes which are not in the vicinity of the surface and Ilan and Loewenthal [27] have shown that the introduction of surface boundary conditions may give rise to instabilities for some range of elastic parameters, even when the previous condition is fulfilled.

Nevertheless, the recursive process, which has been checked together with the method accuracy, is stable for YZ $LiNbO_3$ and for YZ $LiTaO_3$.

3.3. *Determination of Electrical Potentials*

The recursive determination of mechanical displacements requires the knowledge of the electrical potentials at every discrete time. Then, before every incrementation of time, it is necessary to compute these potentials at every node of the study domain.

The potential is governed by an elliptical differential equation, and the finite difference approximation to this piezoelectric coupling equation may be written:

$$\begin{aligned} V(i,j,t) = \frac{1}{2(\epsilon_{11}+\epsilon_{33})}\{&\epsilon_{11}[V(i+1,j,t)+V(i-1,j,t)] \\ &+\epsilon_{33}[V(i,j+1,t)+V(i,j-1,t)] \\ &-[D][\bar{U}'(i+1,j,t)-2\bar{U}'(i,j,t)+\bar{U}'(i-1,j,t)] \\ &-[E][\bar{U}'(i,j+1,t)-2\bar{U}'(i,j,t)+\bar{U}'(i,j-1,t)] \\ &-[F][\bar{U}'(i+1,j+1,t)+\bar{U}'(i-1,j-1,t) \\ &-\bar{U}'(i+1,j-1,t)-\bar{U}'(i-1,j+1,t)]\}, \end{aligned} \tag{26}$$

$$[D] = (e_{11}, 0); \qquad [E] = (e_{35}, e_{33}); \qquad [F] = \left[0, \frac{e_{13}+e_{35}}{4}\right]. \tag{27}$$

Here, the mechanical displacements, already determined at time t, are considered as data, and with respect to potential, this approximation is a "four nodes" type of approximation.

(a) *Dirichlet's problem.* In order to determine the electrical potentials, the problem is modified into a Dirichlet problem by assuming that a zero equipotential is located at a distance d above the surface (Fig. 2). An analytical computation analogous to the one used by Campbell and Jones [2] shows that the change in SAW propagation characteristics is very small when $d \geqslant 0.1\lambda$ (where λ is the wavelength of surface wave), and the initial hypothesis of totally free surface is not altered by the presence of the equipotential. In practice, we have chosen $d = \lambda/2$. Suitable values of potentials are imposed on nodes lying on the artificial boundaries $ABCD$ of the study domain.

In the vacuum above the crystal, the finite difference approximation of Laplace's equation leads to the classical "four nodes" formula.

$$V(i,j,t) = \tfrac{1}{4}[V(i+1,j,t)+V(i-1,j,t)+V(i,j+1,t)+V(i,j-1,t)]. \tag{28}$$

(*b*) *Interface conditions.* Because the derivatives of potential are not continuous across the interface, the centered finite difference approximation (26) and (28) cannot be used for surface nodes. A particular approximation is necessary. This approximation takes into account the piezoelectric coupling equation, Laplace's equation, and mechanical and electrical boundary conditions, and it uses noncentered approximations. For a free surface, it may be written:

$$\begin{aligned} V(0) = \frac{1}{2(\epsilon_{33}+\epsilon_{11}+2\epsilon_0)}\Big\{&2[\epsilon_{33}V(2)+\epsilon_0 V(4)]+(\epsilon_{11}+\epsilon_0)[V(1)+V(3)] \\ &-e_{11}[u_1(1)+u_3(1)-2u_1(0)]-2e_{35}[u_1(2)-u_1(0)] \\ &-2e_{33}[u_3(2)-u_3(0)]+\frac{e_{13}+e_{35}}{2}[u_3(1)+u_3(6)-u_3(3)-u_3(5)] \\ &+\frac{\eta}{\Delta}[u_3(1)-u_3(3)]\Big\}, \end{aligned} \tag{29}$$

with

$$\eta = e_{35}(e_{33}c_{35} - c_{33}e_{35}) + e_{33}(e_{35}c_{35} - c_{55}e_{33}),$$
$$\Delta = c_{33}c_{55} - c_{35}^2, \tag{30}$$

and where the position of a node is characterized by a number, according to the diagram of Fig. 5.

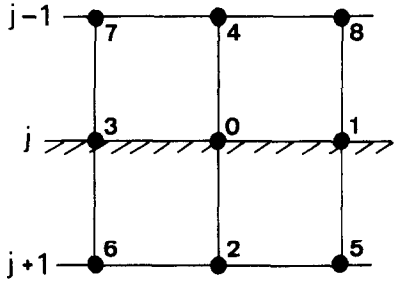

FIG. 5. Characterization of nodes for Eq. (29).

(c) *Linear iterative techniques* [13, 14]. By writing the appropriate finite difference approximation (26) or (28) or (30) at every node (i, j) of the study domain, a linear system is obtained:

$$[A][V] = [B],$$

where the searched potentials at time t, are the elements of column matrix $[V]$

$$V_k = V(i, j, t) \quad \text{with } i = 2, (N-1),\ j = 2, (M-1),\ k = 1, (M-2) \times (N-2). \tag{32}$$

This system is similar to the ones encountered in the finite difference analysis of electrostatic and electromagnetic [28–30] phenomena, though it is more complicated because of coupling between mechanical displacements and potentials. The potentials are then

$$[V] = [A]^{-1}[B]. \tag{33}$$

The matrix A can be inverted by linear iterative techniques. Exact values of potentials are imposed on the boundaries $ABCD$ of the study domain, whereas arbitrary ones V^0 are alloted inside the domain. The appropriate finite difference approximation is applied successively at every node of the study domain, and a new column matrix $V^{(1)}$ is obtained. A new iteration is carried out again and yields $V^{(2)}$. The process converges if $V^{(n)} \to V^{(n-1)}$ as $n \to \infty$.

We have used such techniques in order to determine the potentials at every step of the recursive process, although in order to reduce the number of iterations an overrelaxation method has been chosen [13, 14, 30–32]. With the overrelaxation method, the finite difference approximations (26), (28), and (30) are modified by introducing

a relaxation factor ω. An example of such a modified approximation is given for the Laplace equation:

$$V(i,j,t) = \frac{\omega}{4}[V(i+1,j,t) + V(i-1,j,t) + V(i,j+1,t) + V(i,j-1,t)] - (\omega - 1)\,V(i,j,t). \tag{34}$$

For a study domain of size $M = 240$ and $N = 80$, the optimal value of ω is about 1.77 and the potentials are determined with a precision of about 1% after 18 to 20 iterations. The knowledge of the electrical potentials then allows the incrementation of time and a further computation of mechanical displacements. The linear iterative techniques are used to determine the potentials at every discrete time t.

4. Application of the Numerical Method

4.1. *Initialization*

The numerical simulation of SAW propagation and scattering is initialized by assuming that a pure Rayleigh wave propagates along an unperturbed surface (Fig. 6). At time levels $t = 0$ and $t = 1$, analytically computed values of potentials and displacements due to the pure Rayleigh wave are alloted to nodes of the study domain. At time level $t = 3$, the recursive process is started. Mechanical displacements are computed from the numerical values of potentials and displacements at the two previous times and then the potentials are determined.

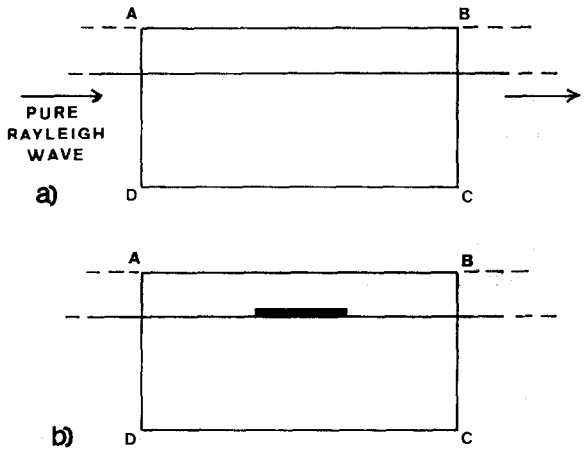

FIG. 6. (a) Initialization: At times $t = 0$ and $t = 1$, it is assumed that a pure Rayleigh wave propagates along an unperturbed surface. (b) After the simulation process has been started, the conditions of the surface perturbation are imposed.

In order to maintain the Rayleigh wave propagation, analytical values in agreement with the initial wave are imposed at every discrete time to nodes lying on the boundaries $ABCD$ of the domain. Thus, the column AD acts as a source, whereas the column BC acts as an "adapted load." When the lower line DC is far enough from the surface, its displacements and potentials can be set to zero.

Boundary conditions corresponding to surface perturbations (metallic strips) are imposed on the surface after the simulation process has been started. Surface wave scattering from discontinuities is numerically simulated, but the recursive process must be stopped just before the scattered waves reach the limits of the domain and consequently the study domain must be chosen long enough.

4.2. *Metallic Strips on Surface*

When metallic strips are layered on the surface, initial solutions are not known and thus the recursive process above is initialized by assuming the surface to be unperturbed at times $t = 0$ and $t = 1$. When the numerical simulations have been started, local appropriate boundary conditions are imposed to surface nodes, i.e., (16), (20) and (21) for a free surface, and (16), (22), and (23) for a metallized surface. However, when the surface is partly metallized, it is necessary to take into account the two electrical conditions which may be imposed onto the strip in order to compute electrical potentials.

(a) *The strip potential is imposed.* If the strip potential denoted by V_s is imposed (generally $V_s = 0$), the value V_s is alloted to surface nodes located at the strip position and this value is maintained unchanged during each linear iterative process.

(b) *The strip potential is not fixed.* This case occurs when the strip is not connected externally (Fig. 7a), or when it is connected to an external electrical circuit, for instance, a resistor between the strip and ground (Fig. 7b). (When $R = 0$, it becomes case (a).) The potential attained by the strip is then a "floating" potential due to the effects of both the surface wave propagation and the electrical circuit (i.e., in the example of Fig. 7b, the latter is given by Ohm's law across the resistor).

Because the piezoelectric crystal is also a dielectric [33], the total electrical charge per unit length of strip must remain unchanged in the case of Fig. 7a, whereas the electrical charge variations are governed by Ohm's law in the case of Fig. 7b. Then,

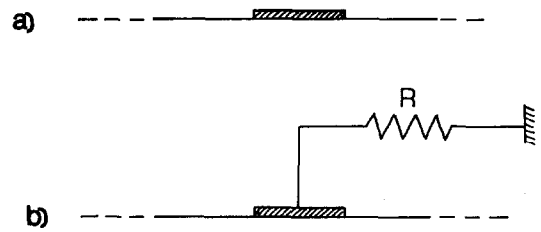

FIG. 7. (a) Unconnected strip. (b) Strip connected to an external electrical circuit. (Here, a resistor between strip and ground.)

at every discrete time, the strip potential V_s is a solution of both the Dirichlet problem and Ohm's law

$$V_s = -R\frac{dQ}{d\tau}, \tag{35}$$

where $dQ/d\tau$ denotes the increase of electrical charge Q per unit length of strip during the time increment $d\tau$.

The finite difference approximation of Ohm's law may be written as

$$Q(t+1) = Q(t-1) - \frac{2l}{R}V_s(t), \tag{36}$$

where the electrical charge $Q(t+1)$ at time $t+1$ is expressed in terms of the strip potential and charge at the two preceding times. (When the strip is insulated, this condition becomes simpler, $Q(t) = 0, \forall t$.)

A particular finite difference approximation is used in order to determine the electrical potential V_s of such strips, i.e., an approximation based upon an application of Gauss' theorem around the strip. Figure 8 shows the grid near a strip. During the

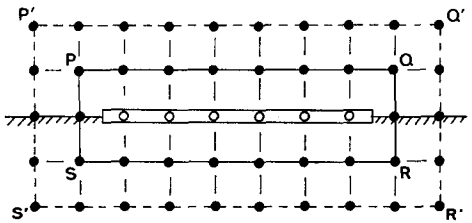

FIG. 8. The grid near a strip. Gauss' theorem across *PQRS* leads to a particular finite difference approximation.

recursive process, the electrical charge per unit length of strip is determined and this charge then acts as input data during the linear iterative resolution of the potentials. Gauss' theorem is applied to the boundary *PQRS* around the strip. Because of the invariance of the solutions along the direction x_2, Gauss' theorem may be written

$$\int_{PQRS} \mathbf{D}.\mathbf{dl} = Q(t), \tag{37}$$

where **D** is the electrical displacement, and **dl** a unit length vector normal to the line *PQRS*.

The writing of a finite difference approximation to D at every node belonging to the boundary *PQRS* yields a difference approximation of V_s,

$$V_s = \frac{Q(t) - q}{(\epsilon_0 + \epsilon_{33})N_s + (\epsilon_0 + \epsilon_{11})}, \tag{38}$$

where N_s is the number of nodes of the strip and q is a linear combination of potentials and displacements of the nodes surrounding the strip (located on lines $PQRS$ and $P'Q'R'S'$). Thus, with the overrelaxation method, the potentials are determined taking into account the electrical conditions.

4.3. *Simulation of SAW Propogation and Scattering*

As a first step, the whole numerical method has been tested for the simplest cases such as the entirely free or the metallized surface. The comparison of numerical results with analytical solutions, well known in these simple cases, has allowed us to determined the precision of the method and, furthermore, to determine the optimal values of the relaxation factor ω.

Most of the numerical calculation has been carried out in a standard study domain in which distances have been normalized with respect to the surface wavelength λ. The size of this standard domain is $M = 240$ and $N = 80$, with a space increment $\lambda/20$ and a time increment $1/60F$, where F is the surface wave frequency. The domain size is thus 12λ long and 4λ deep. The zero equipotential is located at $\lambda/2$ above the surface and the first obstacle is located at 5λ from the line source. The simulation process is stopped after 200 to 260 increments of time, i.e., 3.3 to 4.3 periods. The overrelaxation method requires about 18 iterations when $\omega = 1.77$. The comparison of numerically computed values of u_1, u_3, and V with analytical solutions in the particular case of a free surface leads to an evaluation of the method accuracy. The relative errors on v_r (Rayleigh wave velocity) and on amplitude of vibrations u_1, u_3, and V, after a 3.2 period simulation, are

$$\frac{\Delta v_r}{v_r} = -8 \times 10^{-3}, \qquad \frac{\Delta u_1}{u_1} = -9.5 \times 10^{-3},$$

$$\frac{\Delta u_3}{u_3} = 2.8 \times 10^{-2}, \qquad \frac{\Delta V}{V} = 1.1 \times 10^{-2}.$$

It is seen that the numerical method presented here provides a simulation of SAW propagation in YZ $LiNbO_3$ with good accuracy. It has been used in order to determine SAW behavior near various geometries of electrical discontinuities, each geometry requiring a particular computer run. With the standard study domain size, each computer run is achieved after 180 min *CPU* time with 600K memory size on an IBM 360/65 computer.

Scattering properties of surface acoustic waves are deduced from amplitude curves like the ones presented Figs. 9 and 10. The analysis of such curves leads to reflection and transmission coefficients, whereas the evolution of electrical potentials leads to the characterization of acoustoelectric conversion. Some results thus obtained have been presented already, for example, SAW behavior on a free-metallized interface [15, 16] and on one or two metallic strips [17, 34]. Complete results, concerning both SAW scattering and acoustoelectric conversion, will be pubilshed elswhere and compared to experiments.

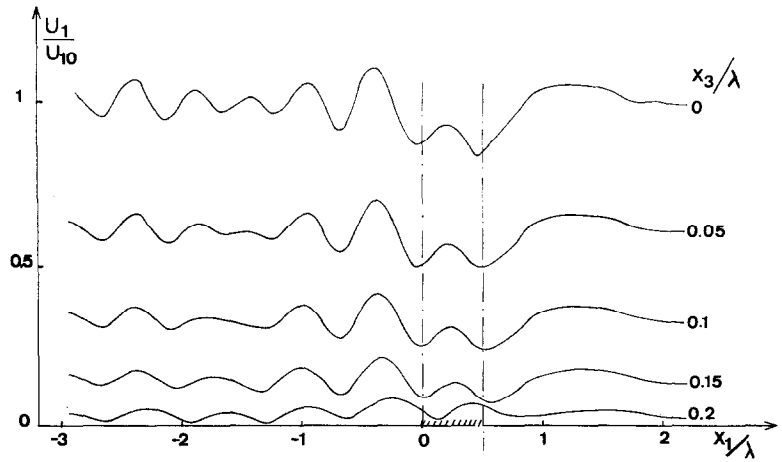

FIG. 9. Example of displacement amplitude curves into the study domain: Amplitude of u_1 in terms of normalized position x_1/λ, x_3/λ. (U_{10} denotes the amplitude of the component u_1 of the incident wave, for $x_3 = 0$.)

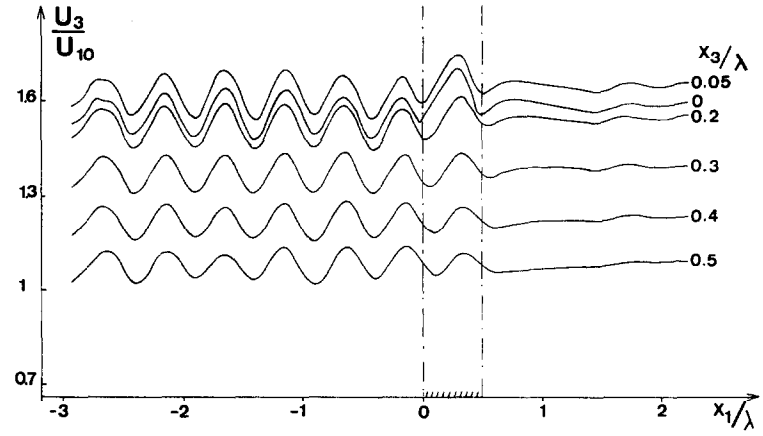

FIG. 10. Example of amplitude curves: Amplitude of u_3 in terms of normalized position x_1/λ, x_3/λ.

5. CONCLUSION

A finite difference analysis of SAW propagation and scattering on a highly piezoelectric *YZ* $LiNbO_3$ crystal has been presented. This analysis, which uses two different techniques in order to solve the coupled electromechanical equation in piezoelectric materials, is well suited to the simulation of the SAW behavior near surface perturbations, and it may be considered as a useful analytic tool. It should be improved further in order to be available for any crystal cut and any direction of propagation.

ACKNOWLEDGMENTS

This work was supported by the "Centre d'études et de Recherches I.B.M. La Gaude," La Gaude, France. We wish to thank MM. A. Desblache and J. Monrolin for their helpful suggestions and encouragement.

REFERENCES

1. J. D. MAINES AND E. G. S. PAIGE, *Proc. IEE* **120**, No. 10R (1973), 1078.
2. J. J. CAMPBELL AND W. R. JONES, *IEEE Trans. Sonics Ultrason. SU*-**15**, No. 4 (1968), 209.
3. Z. ALTERMAN AND A. ROTENBERG, *Bull. Seismol. Soc. Amer.* **59**, No. 1 (1969).
4. Z. ALTERMAN AND D. LOEWENTHAL, *Geophys. J. Roy. Soc.* **20** (1970), 101.
5. M. MUNASINGHE AND G. W. FARNELL, *in* "1972 Ultrasonics Symposium," p. 267, IEEE Cat. 72 CHO 708-8SU, 1972.
6. M. MUNASINGHE AND G. W. FARNELL, *J. Appl. Phys.* **44**, No. 5 (1973).
7. M. MUNASINGHE AND G. W. FARNELL, *J. Geophys. Res.* **78**, No. 14 (1973), 2454.
8. E. CAMBIAGGIO, F. CUOZZO, AND E. RIVIER, *in* "Proceedings of the Fifth Colloquium on Microwave Communication," Akadémiai Kiado, Budapest, June 1973, ET-11.
9. E. CAMBIAGGIO, F. CUOZZO, J. P. DAMIANO, AND E. RIVIER, *in* "Proceedings of the 1975 International Microwave Symposium," p. 362, IEEE Cat. 75 CHO955-5, 1975.
10. F. CUOZZO, E. CAMBIAGGIO, J. P. DAMIANO, AND E. RIVIER, *IEEE Trans. Sonics Ultrason. SU*-**24**, No. 3 (1977), 280.
11. J. P. DAMIANO AND E. RIVIER, *in* "Proceedings of the 1977 Ultrasonics Symposium," IEEE Cat. No. 77 CH1264-1SU, 1977.
12. R. D. RICHTMYER, "Difference Method for Initial Value Problem," Interscience, New York, 1957.
13. J. GIRERD AND W. J. KARPLUS, "Traitement des équations différentielles sur calculateur électronique," Gauthier–Villars, Paris, 1968.
14. G. E. FORSYTHE AND W. R. WASOW, "Finite Difference Methods for Partial Differential Equations," Wiley, New York, 1960.
15. E. CAMBIAGGIO AND F. CUOZZO, *in* "1975 Ultrasonics Symposium Proceedings," p. 444, IEEE Cat. No. 75 CH0994-4SU, 1975.
16. E. CAMBIAGGIO, F. CUOZZO, AND E. RIVIER, *Appl. Phys. Lett.* **22**, No. 2 (1976), 71.
17. E. CAMBIAGGIO, F. CUOZZO, AND E. RIVIER, *in* "1976 Ultrasonics Symposium Proceedings," IEEE Cat. No. 76 CH1120-5SU, 1976.
18. G. CAMBON AND Q. F. QUATE, *Electron. Lett.* **5** (1969), 402.
19. G. W. FARNELL AND E. L. ADLER, *in* "Physical Acoustics" (W. P. Mason and R. N. Thurston, Eds.), Vol. 9, Academic Press, New York/London, 1972.
20. H. F. TIERSTEN, *J. Appl. Phys.* **20**, No. 2 (1969), 770.
21. G. W. FARNELL, *in* "Physical Acoustics" (W. P. Mason and R. N. Thurston, Eds.), Vol. 6, Academic Press, New York/London, 1970.
22. W. R. SMITH, H. M. GERARD, J. H. COLLINS, T. M. REEDER, AND H. J. SHAW, *IEEE Trans. Microwave Theory Tech. MTT*-**17**, No. 11 (1969), 856.
23. W. R. SMITH, H. M. GERARD, J. H. COLLINS, T. M. REEDER, AND H. J. SHAW, *IEEE Trans. Microwave Theory Tech. MTT*-**17**, No. 11 (1969), 865.
24. B. A. AULD, "Acoustic Fields and Waves in Solids," Wiley, New York/London, 1973.
25. A. W. WARNER, M. ONOE, AND G. A. COQUIN, *J. Acoust. Soc. Amer.* **42**, No. 6 (1967), 1223.
26. J. F. NYE, "Physical Properties of Crystals," Oxford Univ. Press (Clarendon), London/New York, 1957.
27. A. ILAN AND D. LOEWENTHAL, *Geophys. Prospect. XXIV*, No. 3 (1976), 431.
28. H. E. BRENNER, *IEEE Trans. Microwave Theory Tech. MTT*-**15**, No. 8 (1967).

29. D. H. SINNOTT, G. K. CAMBRELL, C. T. CARSON, AND H. E. GREEN, *IEEE Trans. Microwave Theory Tech. MTT*-**17**, No. 8 (1969), 464.
30. R. DAUMAS, D. POMPEI, E. RIVIER, AND A. ROS, *IEEE Trans. Microwave Theory Tech. MTT*-**21**, No. 8 (1973), 552.
31. S. P. FRANKEL, *M.T.A.C.* **4** (1950), 65.
32. D. M. YOUNG, *Trans. Amer. Math. Soc.* **76** (1954), 92.
33. G. A. COQUIN AND H. F. TIERSTEN, *J. Acoust. Soc. Amer.* **41**, No. 4 (1967), 921.
34. F. CUOZZO AND E. CAMBIAGGIO, *in* "Proceedings of the Colloque National sur le Traitement du signal et ses Applications, Nice, France, April 26–30, 1977."